

# 1 Solvent engineering of MAPbI<sub>3</sub> perovskite thick film for direct 2 X-ray detector

Wei Qian<sup>a,b</sup>; Weitao Qiu<sup>a</sup>; Shanshan Yu<sup>a,c</sup>; Duan Huang<sup>a</sup>; Renbo Lei<sup>b</sup>; Xianzhen  
Huang<sup>a</sup>; Shuang Xiao<sup>a</sup>; Xinwei Wang<sup>\*b</sup>; Shihe Yang<sup>\*a,c</sup>

<sup>5</sup> <sup>a</sup> *Guangdong Provincial Key Lab of Nano-Micro Materials Research, School of  
6 Chemical Biology and Biotechnology, Shenzhen Graduate School, Peking  
7 University, Shenzhen, Guangdong 518055, China.*

<sup>8</sup> <sup>b</sup> School of Advanced Materials, Shenzhen Graduate School, Peking University,  
<sup>9</sup> Shenzhen 518055, China;

<sup>10</sup> <sup>c</sup> Institute of Biomedical Engineering, Shenzhen Bay Laboratory, Shenzhen,  
<sup>11</sup> Guangdong 518107, China

12 Email: [wangxw@pkusz.edu.cn](mailto:wangxw@pkusz.edu.cn)

13 Email: [chsyang@pku.edu.cn](mailto:chsyang@pku.edu.cn)

14

15

16

17

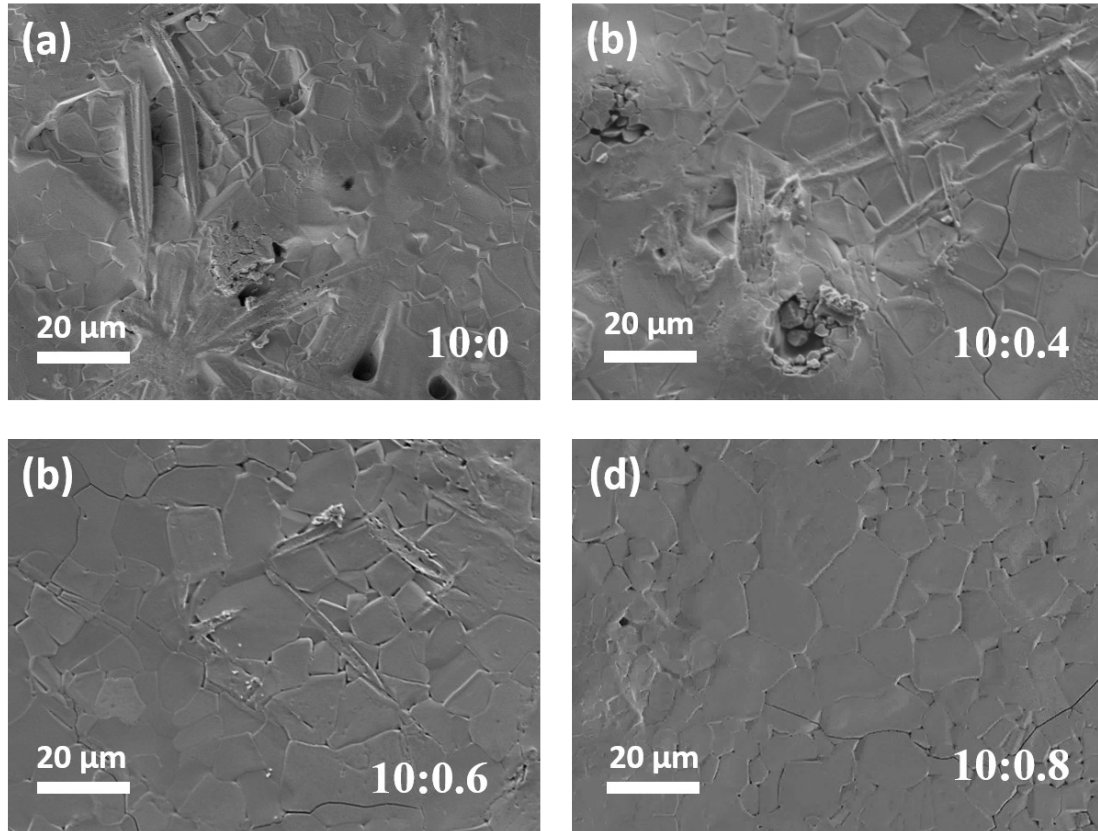
18

10

20

21

22



23

24      Figure. S1 Top-view SEM images of perovskite films prepared from precursor  
25      solution with different mixing ratio of DMSO and ethylene glycol.

26

27

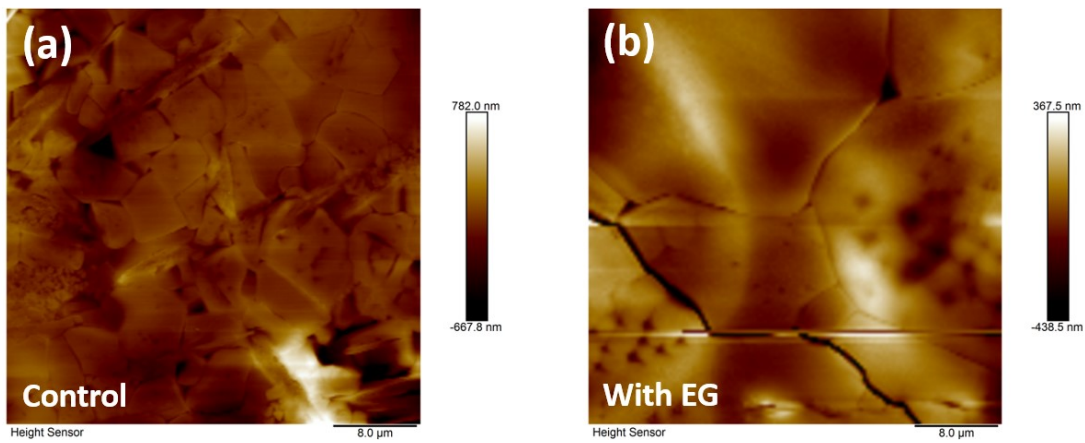
28

29

30

31

32



33

34      Figure.S2 The AFM images of the control (a) and experimental sample (b).

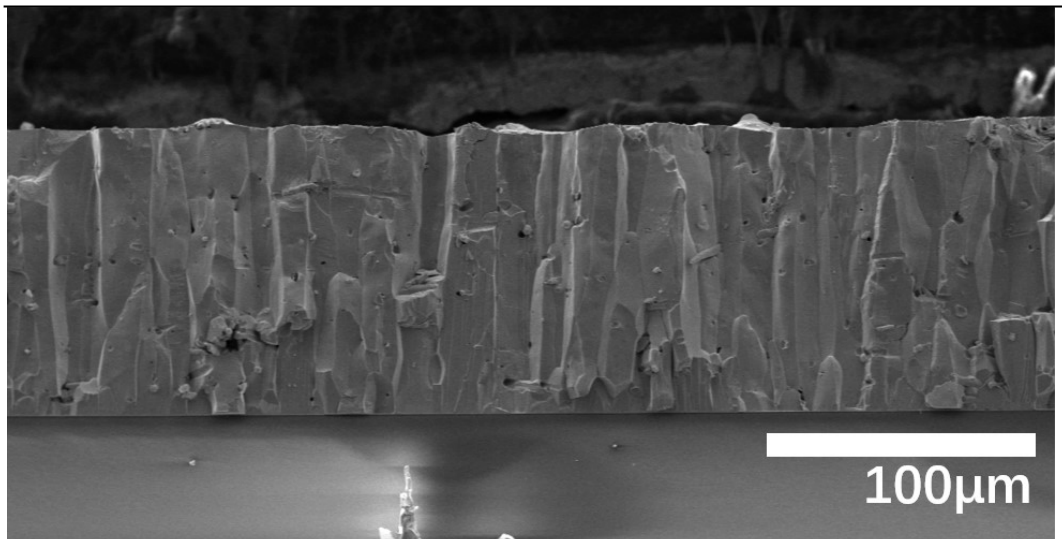
35

36

37

38

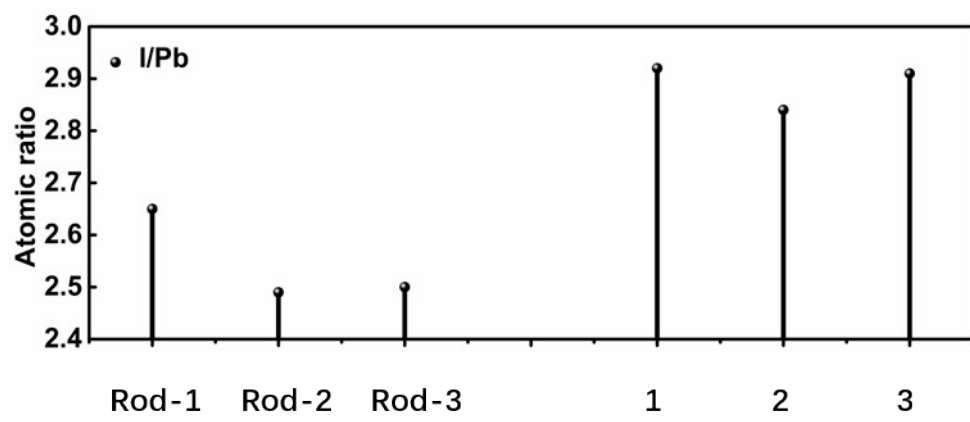
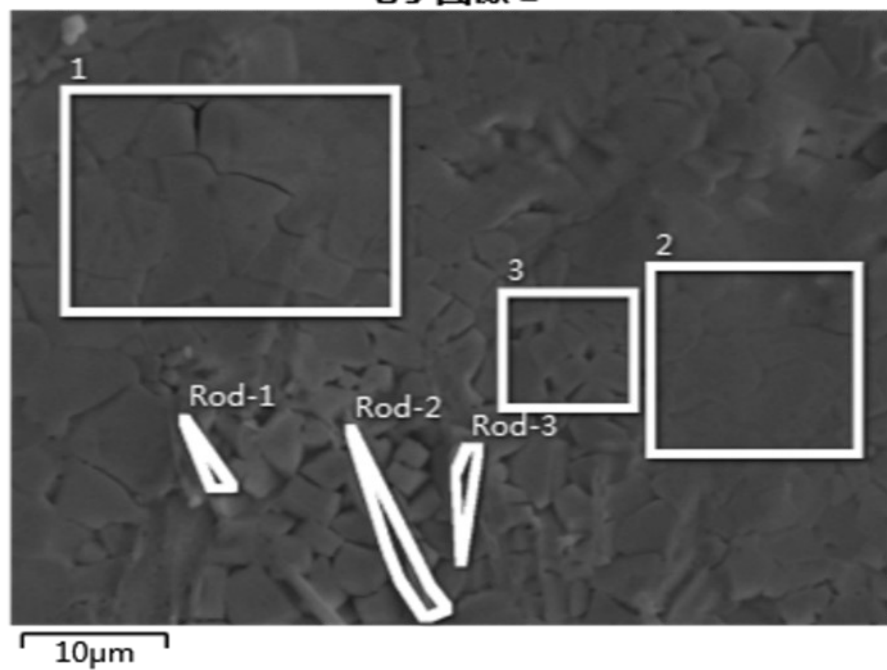
39



40

41      Figure.S3 The cross section SEM images of the 100 $\mu\text{m}$  perovskite films  
42      (experimental sample).

电子图像 2



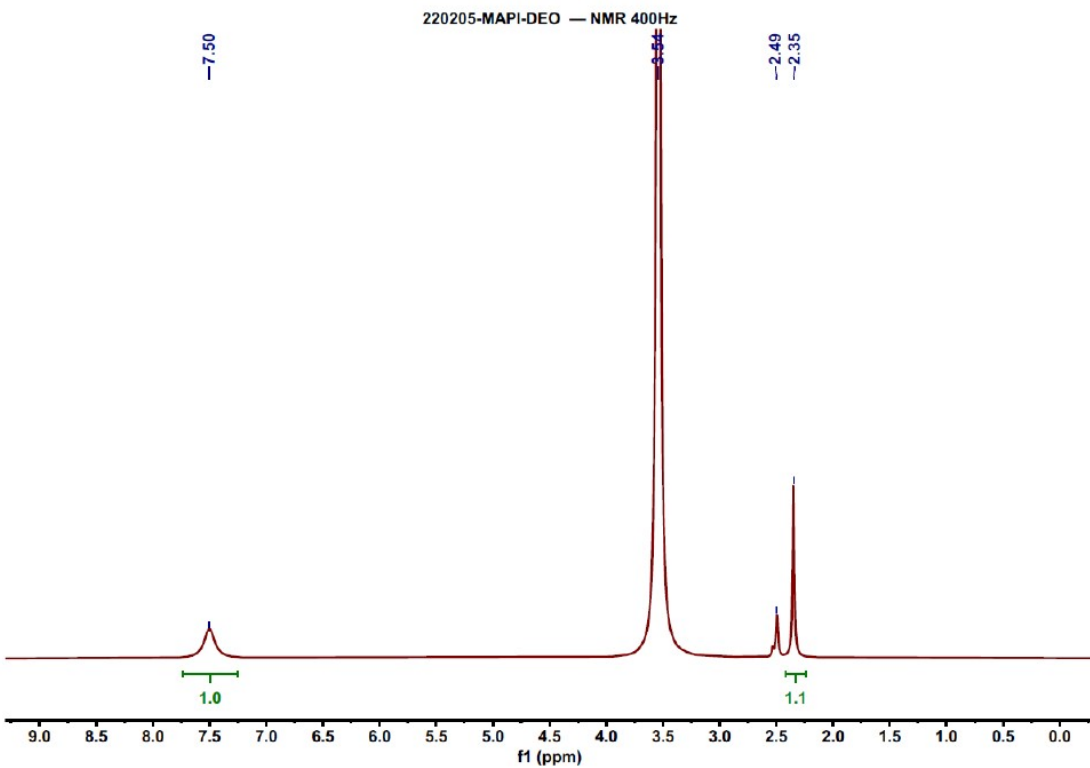
43

44 Figure. S4. EDS Analysis for different areas on the surface of perovskite films in the  
45 Control Group.

46

47

48



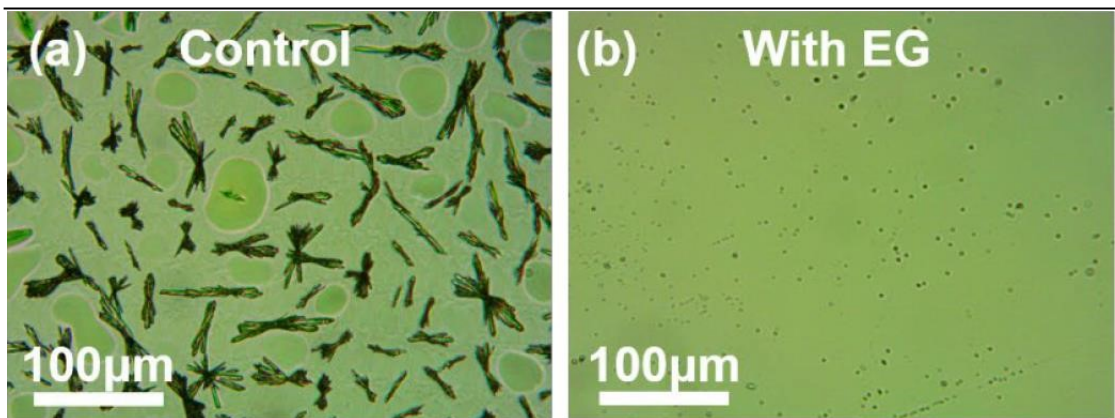
50 Figure.S5 The perovskite film of experimental group was dissolved in DMSO solvent  
51 for NMR analysis

52

53

54

55



56

57 Figure.S6 In-situ optical microscopy images of the control and experimental wet films  
58 prepared by spin-coating method.

59

60

61

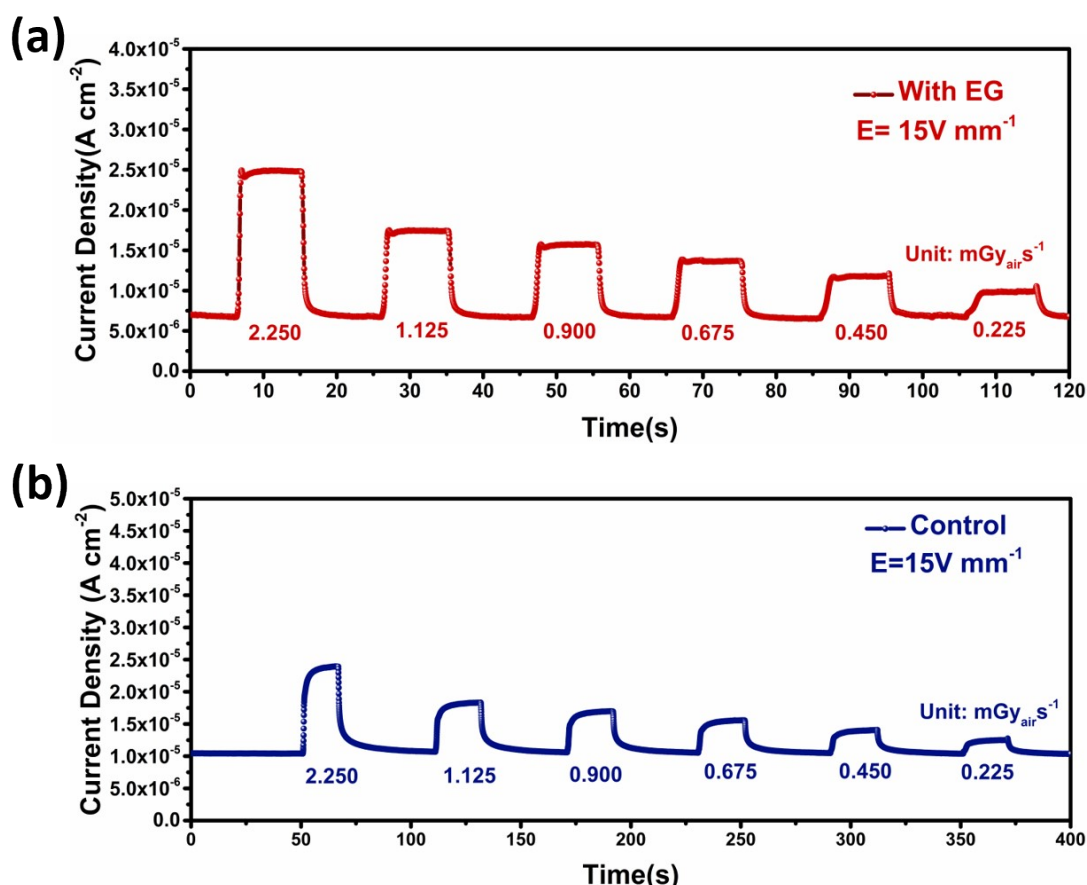
62

63

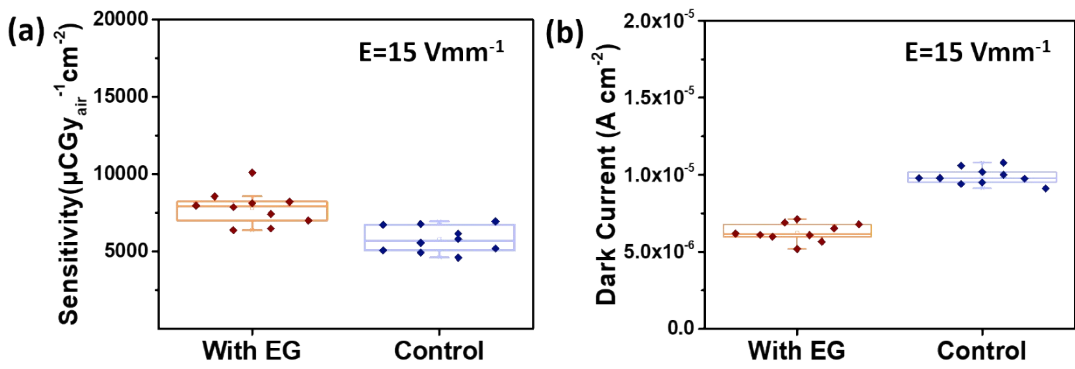
64

65

66



69 Figure. S7 (e) The X-ray response profiles of the control and experimental detectors  
70 with a varying dose rate ranging from  $2.25 \text{ mGy}_{\text{air}} \text{s}^{-1}$  to  $0.225 \text{ mGy}_{\text{air}} \text{s}^{-1}$ .



74

75      Figure. S8 (a) Box map of the sensitivity of 10 samples in experimental group and  
76      control group. (b) Box map of the dark current of 10 samples in experimental group  
77      and control group.

78

79

80

81

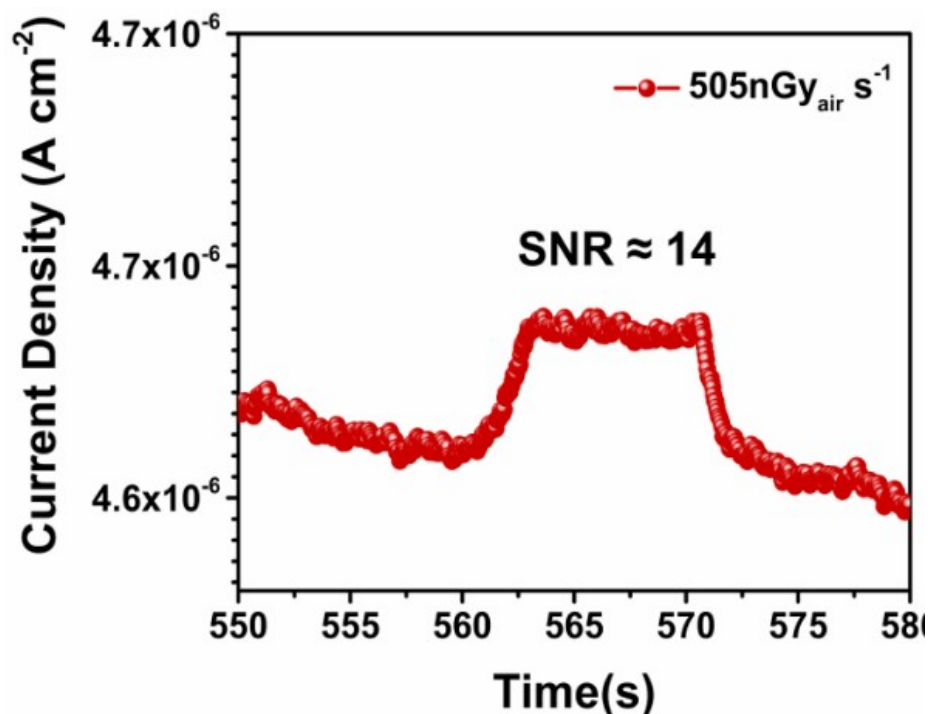
82

83

84

85

86



87

88 Figure.S9 The X-ray response of the double-layer perovskite detector at an ultralow  
89 dose of  $550 \text{ nGy}_{\text{air}} \text{s}^{-1}$ .

90

91

92

93

94

95

Table S1 Key parameters of the X-ray detectors made of perovskite materials

Device Structure	$E_{ph}$ (keV)	$E$ (V mm <sup>-1</sup> )	$S$ ( $\mu\text{CGy}_{\text{air}}^{-1}\text{cm}^{-2}$ )	LoD (nGy <sub>air</sub> s <sup>-1</sup> )	Ref.
Au//CsPbBr <sub>3</sub> /Au	50	20	918		60
Au//RbCsPbBr <sub>3</sub> /Au	50	20	8097		60
Au/(BA) <sub>2</sub> EA <sub>2</sub> Pb <sub>3</sub> Br <sub>10</sub> /Au	70	5	$6.8 \times 10^3$	5500	61
Au/Cs <sub>2</sub> AgBiBr <sub>6</sub> /Au	50	50	1974	45.7	62
Au/PEA-Cs <sub>2</sub> AgBiBr <sub>6</sub> /Au	50	23	288.8		62
Au/(BA) <sub>2</sub> CsA <sub>g</sub> BiBr <sub>7</sub> /Au	70	5	4.2		63
Ag/(H <sub>2</sub> MDAP)BiI <sub>5</sub> /Ag	70	5	1		64
PEN/NiO <sub>x</sub> / Cs <sub>0.1</sub> FA <sub>0.75</sub> MA <sub>0.15</sub> PbBr <sub>0.5</sub> I <sub>2.5</sub> /PCBM/ BCP/Au	70	27	33.5	12000	38
ITO/Pt/Polymer/CsPbBr <sub>3</sub> / W	70	45.5	$1.2 \times 10^4$		65
ITO/TiO <sub>2</sub> /Cs <sub>2</sub> TeI <sub>6</sub> /PTAA/Au	60	50	0.24		66
FTO/MAPbI <sub>3</sub> /C	60	15	7304	154	This work